

Multielectron photoexcitations in x-ray-absorption spectra of 4*p* elements

J. Padežnik Gomilšek,¹ A. Kodre,^{2,3} I. Arčon,^{2,4} A. M. Loireau-Lozac'h,⁵ and S. Bénazeth^{6,7}

¹*Faculty of Mechanical Engineering, University of Maribor, Maribor, Slovenia*

²*J. Stefan Institute, Jamova 39, 1001 Ljubljana, Slovenia*

³*Faculty of Mathematics and Physics, University of Ljubljana, Ljubljana, Slovenia*

⁴*Nova Gorica, Polytechnic, Nova Gorica, Slovenia*

⁵*Laboratoire de Chimie Physique et de Chimie Minérale, Faculté des Sciences Pharmaceutiques et Biologiques, Université René Descartes, Paris, France*

⁶*Laboratoire pour l'Utilisation du Rayonnement Electromagnétique (LURE), Université Paris-Sud, F91405 Orsay, France*

⁷*Laboratoire de Biomathématique, Faculté de Pharmacie, Université Paris V, Paris, France*

(Received 19 October 1998)

By removing the structural x-ray-absorption fine-structure signal from *K*-edge absorption spectra of 4*p* elements from Ga to Br in chalcogenide glasses and other samples, the pure atomic absorption is recovered. Its main components are shake-up and shake-off channels of the [1*s*3*p*] and [1*s*3*d*] group. The [1*s*3*p*]4*p* shake-up channel is observed to close off along the series as the 4*p* shell is progressively filled.
[S1050-2947(99)05804-7]

PACS number(s): 32.30.Rj, 32.80.Fb, 78.70.Dm

Tiny features superposed onto the smooth variation of an x-ray photoabsorption cross section with energy above inner-shell absorption edges are fingerprints of multielectron excitations (MPE) [1]. They have been studied extensively since they provide information on the correlated motion of electrons in an atomic system, indispensable in testing advanced theoretical models [2–6]. The complete spectrum of MPE accompanying an inner-shell photoeffect has only been measured on monatomic samples of noble gases and some metals in a vapor state [1,6–11]. For elements which cannot be conveniently prepared in a monatomic state, the structural x-ray-absorption fine-structure (XAFS) component in absorption spectra prevails, and masks the small MPE component. Efforts to separate the two components reliably have recently been evident in both fields of research: In atomic physics [12–18], the aim is to extend the experimental data on MPE to majority of elements. In the XAFS field, on the other side, the MPE spectrum represents the so-called atomic background to the structural signal [19–23]. The empirical models currently in use are recognized as the major source of uncertainty in precision structural analysis [20,22].

The techniques to separate the MPE and XAFS components rely on the different basic properties of the two effects: The XAFS signal is a superposition of harmonic components which can be modeled from the known arrangement of atoms. The atomic MPE signal is composed of distinct absorption features such as resonances and absorption edges, and consequently much more difficult to predict with comparable precision. However, it is expected to change smoothly between neighbor elements, so that a good approximation can be obtained by interpolating the data from a few elements to an entire series with a similar shell structure as, e.g., lanthanide series [18], and third- [24] and fifth-period elements [25]. The main source of uncertainty in the separation comes from spurious harmonic components generated by the MPE signal. Thus, within a single absorption spectrum, the two components can only be partially separated in the best cases

[12,13]. A complete analysis can be implemented with additional information [13–15]. We show that it can be achieved by combining information from different samples of the same element, presupposing the transferability of the MPE signal. This technique has been demonstrated in the case of Rb, where a pure atomic spectrum of Rb vapor has been used as an approximation of the Rb⁺-ion MPE signal in aqueous solution of Rb salts [22]. In a similar approach, separation of the MPE signal using solely Rb⁺-ion samples has proved successful [26].

In general, when an approximate XAFS signal is determined for a sample and subsequently eliminated from the absorption spectrum, the residual contains the atomic absorption, the contribution of the unresolved XAFS components and the noise of the experiment. This residual can be used as an approximate atomic absorption background for another sample, to yield, after subtraction, the basis for an improved XAFS model. Iterating the procedure between the two samples results in refined XAFS models and the common atomic background. The convergence, however, depends crucially on the degree of order in the structure of the samples. It is found that both extreme cases of order result in slow convergence. For highly ordered samples, such as, e.g., crystalline Ge, the structural parameters are well known and a precise *ab initio* XAFS model can be built in the FEFF code [27] with hundreds of photoelectron scattering paths. However, approximations inherent to the FEFF models and the necessary truncation of the path series introduce a strong contribution of the structural signal into the residual. On the other hand, for highly disordered samples, typically in a liquid state, the structural signal can be relatively simple, but the structure parameters are not known in advance and the XAFS model can only be built by fitting the data so that the danger of absorbing MPE contribution into spurious structural components cannot be avoided.

Best results have been obtained with partly disordered samples. For most 4*p* elements, the chalcogenide glasses

TABLE I. The list of the employed samples with references to the structure and/or experimental procedure.

Z	Sample	Ref.
31	6Ge ₂ S ₄ -4Ga ₂ S ₃	glass [28]
31	3Ga ₂ S ₃ -Ga ₂ Te ₃	glass [28]
32	9Ge ₂ S ₄ -Ga ₂ S ₃	glass [28]
32	Ge(CH ₃) ₄	vapor
32	Ge	crystalline
32	GeO ₂	crystalline
33	AsS	glass [29]
33	AsTe ₄	glass [30]
33	As	vapor
34	Se	glass [31]
34	Se ₇ -Te ₃	glass [31]
35	KBr	aqueous solution [26]
35	CTAB	on carbon black [32]
36	Kr	gas

were found as ideal starting cases: their rigid basic units of the structure, the chalcogenide tetrahedra, form a rather disordered framework [28,30,31]. Thus the XAFS signal consists mainly of the contribution of the nearest neighbors, which can be modeled with sufficient accuracy, while the signal from further neighbors largely cancels out. For the other sample in the iteration procedure, crystalline and amorphous materials, as well as molecular gases were used (Table I). The case of Br, for which no chalcogenide glass exists, is described elsewhere [26]. The spectra were measured at synchrotron facilities at Laboratoire pour l'Utilisation du Rayonnement Electromagnétique (LURE) (beamline D42), Hamburger Synchrotronstrahlungslabor (HASYLAB) (X1.1, BW1) and European Synchrotron Radiation Facility (ESRF) (BL29). Typical experimental parameters of the beamlines have been described in earlier publications [10,17,32].

The procedure provides the MPE atomic background signal which optimizes the XAFS signal of two independent samples of a given element. The results for Ge (Fig. 1) show

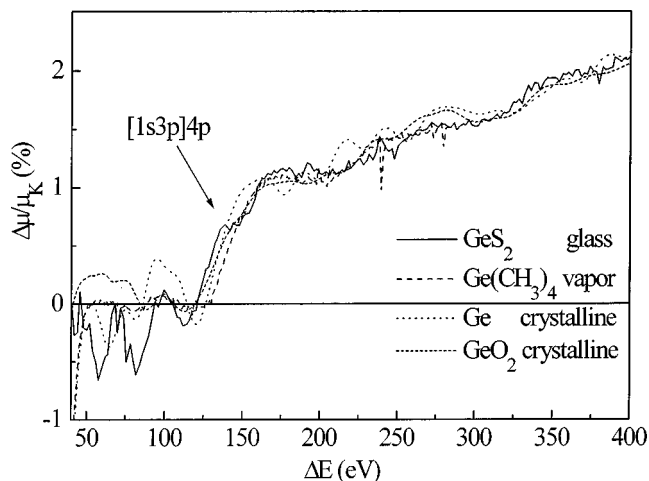


FIG. 1. The $[1s3p]$ MPE group contribution to the Ge photoabsorption from residuals of different Ge samples. The origin of the energy scale is set at the $[1s]$ threshold.

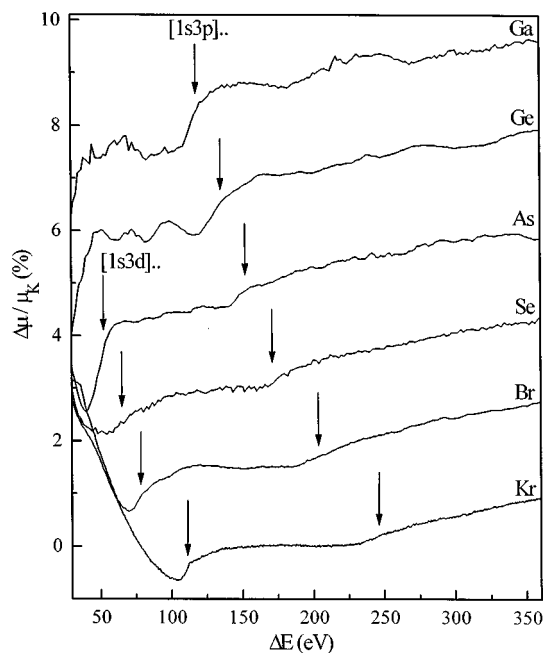


FIG. 2. The contribution of the $[1s3p]$ MPE group in elements from Ga to Kr. The HF energy estimates of the lowermost resonance in a group are indicated by arrows. For elements from As to Kr the $[1s3d]$ group contribution is also resolved. A relative energy scale as in Fig. 1 is used.

that the residuals for different sample pairs agree in the essential ingredient: although the MPE signal retains most of the experimental noise and some of the unresolved structural components, the prominent step attributed to the $[1s3p]4p$ MPE appears with the same amplitude and width in all cases,

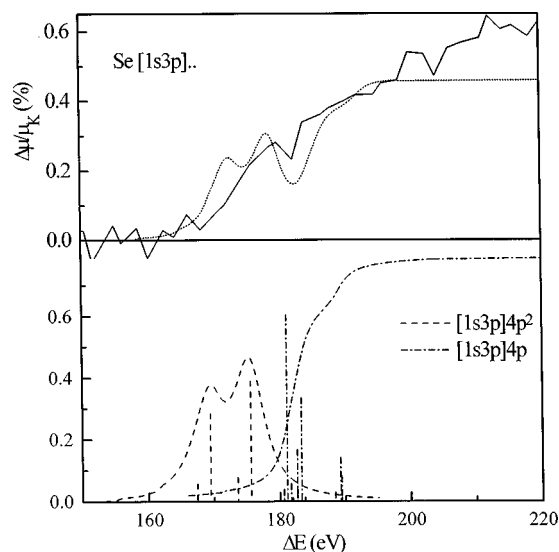


FIG. 3. Above: the comparison of experimental (solid) and theoretical values (short dotted) of the $[1s3p]$ MPE group contribution in Se. Below: the calculated relative transition probabilities to the $[1s3p]4p^2$ (dashed) and $[1s3p]4p$ (dash-dotted) multiplets are shown as vertical lines. The corresponding spectral distributions are obtained by convolution with a Lorentzian of 5-eV width, close to the total lifetime width. The match with experimental data requires a 3-eV shift of the calculated energies and an amplitude adjustment factor of 0.6.

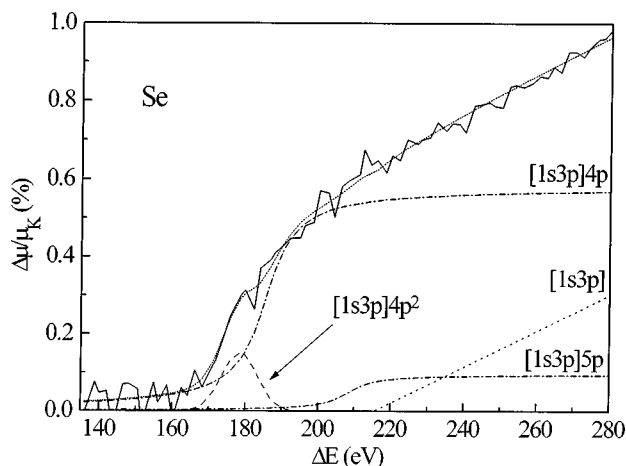


FIG. 4. Best-fit decomposition of the measured $[1s3p]$ MPE group into the contributions of the $[1s3p]4p^2$ resonance, the $[1s3p]4p$ and $[1s3p]5p$ shake-up edges, and the $[1s3p]$ shake-off. Relative energies of the components are kept fixed at the multiplet averages from the HF calculation.

and close to the energy estimated by Hartree-Fock (HF) calculation [33]. Similarly, the results for the entire series of elements (Fig. 2) show agreement with the HF calculation in the steady progression of threshold energies. For elements above As, the $[1s3d]$ MPE closer to the K edge is also resolved.

A more rigorous test of the experimental results than the mere agreement with HF energies is provided by a theoretical estimate of the excitation cross section. The calculation was performed with fully relaxed Dirac-Fock orbitals [4,34]. The result is shown in Fig. 3 for the case of $[1s3p]$ excitation in Se. Although the experimental resolution is too coarse to show the effect of the multiplet splitting of the resonant and shake-up transition, the agreement in the overall shape, after a modest adjustment in the energy and intensity scale, is satisfactory. Mainly the calculation shows, in the vein of a similar analysis on Kr [6], which reaction channels contribute to the observed spectral feature. In the present case, the resonant double excitation to the $[1s3p]4p^2$ state has a comparable amplitude to the shake-up transition, although no resonant peak is observed: however, the presence of the resonance shifts the apparent shake-up edge to lower energy. In addition, to the $[1s3p]4p$, shake-up the $[1s3p]5p$ shake-up also contributes appreciably, extending the apparent width of the edge.

With this information, the detected $[1s3d]$ and $[1s3p]$ MPE features are decomposed with an *ad hoc* ansatz into a resonant contribution and two shake-up edges. The observed change of slope on both sides of a feature is attributed to the shake-off transitions, where the cross section grows linearly with the excess energy above the threshold [6]. The result of the decomposition for Se is shown in Fig. 4, and the amplitudes of the components for the entire element series in Fig. 5. Evidently, the transition probabilities to the individual excitation channels are governed mainly by the number of accessible orbitals for the excited electron(s) [25]: hence the linear trend in the $[1s3p]4p$ cross section and the constant cross section of the $[1s3p]5p$ channel. Even the resonant $[1s3p]4p^2$ cross section, in spite of the rather large uncer-

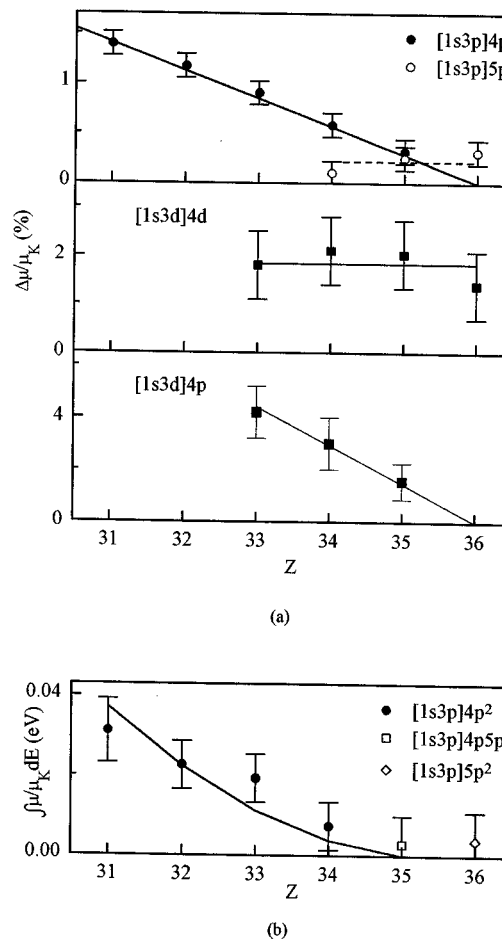


FIG. 5. The relative magnitudes of $[1s3p]$ and $[1s3d]$ photo-absorption channels along the series of the $4p$ elements. Solid lines show the expected dependence on the number of accessible $4p$, $5p$, and $4d$ orbitals. (a) Asymptotic magnitude of the shake-up channels. (b) Integrated intensity of the resonant channels.

tainty interval, shows a convincingly quadratic trend, i.e., a proportionality to the number of pairs of accessible $4p$ orbitals. Similar conclusions are found for the shorter series of the $[1s3d]$ excitations.

Although the data on the MPE energies and cross sections extracted in the present analysis cannot compete with those from monatomic samples in sensitivity and resolution, the method can be applied generally for a systematic investigation of most elements in the Periodic Table. In addition, the results of the analysis offer some insight into the excitation mechanism. The simple dependence of the decomposed cross-section contributions on the number of the accessible orbitals in the final state suggests that the matrix elements for different channels change only slightly from element to element. This is an indication that the indirect, shake, mechanism could be sufficient for the description of the process.

Support of the Slovenian Ministry of Science and Technology and Internationales Büro Jülich (Germany) is acknowledged. L. Troeger and R. Frahm of HASYLAB and A. Filipponi of ESRF (BL29) provided expert advice on beam-line operation.

- [1] D. Deslattes, R. E. LaVilla, P. L. Cowan, and A. Henins, *Phys. Rev. A* **27**, 923 (1983).
- [2] H. P. Saha, *Phys. Rev. A* **42**, 6507 (1990).
- [3] W. Cooper, *Phys. Rev. A* **38**, 3417 (1988).
- [4] M. Štuhec, A. Kodre, M. Hribar, I. Arčon, D. Glavič-Cindro, and W. Drube, *Phys. Rev. A* **49**, 3104 (1994).
- [5] R. L. Martin and D. A. Shirley, *J. Chem. Phys.* **64**, 3685 (1976).
- [6] S. J. Schaphorst, A. F. Kodre, J. Ruscheinski, B. Crasemann, T. Åberg, J. Tulkki, M. H. Chen, Y. Azuma, and G. S. Brown, *Phys. Rev. A* **47**, 1953 (1993).
- [7] M. Deutsch, N. Maskil, and W. Drube, *Phys. Rev. A* **46**, 3963 (1992).
- [8] M. Deutsch, G. Brill, and P. Kizler, *Phys. Rev. A* **43**, 2591 (1991).
- [9] I. Arčon, A. Kodre, M. Štuhec, D. Glavič-Cindro, and W. Drube, *Phys. Rev. A* **51**, 147 (1995).
- [10] R. Prešeren, I. Arčon, M. Mozetič, A. Kodre, and A. Pregelj, *Nucl. Instrum. Methods Phys. Res. B* **111**, 161 (1996).
- [11] A. Filipponi, L. Ottaviano, and T. A. Tyson, *Phys. Rev. A* **48**, 2098 (1993).
- [12] G. Li, F. Bridges, and G. S. Brown, *Phys. Rev. Lett.* **68**, 1609 (1992).
- [13] P. D'Angelo, A. Di Cicco, A. Filipponi, and N. V. Pavel, *Phys. Rev. A* **47**, 2055 (1993).
- [14] P. D'Angelo, H.-F. Nolting, and N. V. Pavel, *Phys. Rev. A* **53**, 798 (1996).
- [15] P. D'Angelo, A. Di Nola, E. Giglio, M. Mangoni, and N. V. Pavel, *J. Phys. Chem.* **99**, 5471 (1995).
- [16] A. Kodre, I. Arčon, M. Hribar, M. Štuhec, and F. Villain, *J. Phys. (Paris), Colloq.* **4**, C9-397 (1994).
- [17] A. Kodre, I. Arčon, M. Hribar, M. Štuhec, F. Villain, W. Drube, and L. Troeger, *Physica B* **208&209**, 379 (1995).
- [18] J. A. Solera, J. Garcia, and M. G. Proietti, *Phys. Rev. B* **51**, 2678 (1995).
- [19] J. J. Chaboy, A. Marcelli, and T. A. Tyson, *Phys. Rev. B* **49**, 11 652 (1994).
- [20] A. Filipponi, *Physica B* **208&209**, 29 (1995).
- [21] A. Di Cicco, *Physica B* **208&209**, 125 (1995).
- [22] A. Kodre, I. Arčon, and R. Frahm, *J. Phys. (Paris), Colloq.* **7**, C2-195 (1997).
- [23] I. Arčon and A. Kodre, *J. Phys. (Paris), Colloq.* **7**, C2-233 (1997).
- [24] A. Filipponi, T. A. Tyson, K. O. Hodgson, and S. Mobilio, *Phys. Rev. A* **48**, 1328 (1993).
- [25] A. Filipponi and A. di Cicco, *Phys. Rev. A* **52**, 1072 (1995).
- [26] A. Kodre, J. Padežnik Gomilšek, I. Arčon, and R. Prešeren, *J. Synchrotron Radiat.* (to be published).
- [27] E. A. Stern, M. Newville, B. Ravel, Y. Yacoby, and D. Haskel, *Physica B* **208&209**, 117 (1995); J. J. Rehr, R. C. Albers, and S. I. Zabinsky, *Phys. Rev. Lett.* **69**, 3397 (1992).
- [28] A. M. Loireau-Lozac'h, F. Keller-Besrest, and S. Bénazeth, *J. Solid State Chem.* **123**, 60 (1996).
- [29] C. Y. Yang, M. A. Paesler, and D. E. Sayers, *Phys. Rev. B* **39**, 10 342 (1989).
- [30] Q. Ma, D. Raoux, and S. Bénazeth, *Phys. Rev. B* **48**, 16 332 (1993).
- [31] M. Majid, J. Purans, S. Bénazeth, and C. Souleau, *J. Phys. IV* **7**, 1155 (1997).
- [32] M. Bele, A. Kodre, I. Arčon, J. Grdadolnik, S. Pejovnik, and J. O. Besenhard, *Carbon* **36**, 1207 (1998).
- [33] C. Froese-Fischer, *Comput. Phys. Commun.* **43**, 355 (1987).
- [34] K. G. Dyall, I. P. Grant, C. T. Johnson, F. A. Parpia, and E. P. Plummer, *Comput. Phys. Commun.* **55**, 425 (1989).